Kinetic and paramagnetic NMR investigations of the inhibition of Streptomyces antibioticus tyrosinase

Bubacco, L.; Vijgenboom, E.; Gobin, C.; Tepper, A.W.J.W.; Salgado, J.; Canters, G.W.

ELSEVIER

Journal of Molecular Catalysis B: Enzymatic 8 (2000) 27–35

JOURNAL OF MOLECULAR CATALYSIS B: ENZYMATIC

www.elsevier.com/locate/molcatb

Kinetic and paramagnetic NMR investigations of the inhibition of *Streptomyces antibioticus* tyrosinase

Luigi Bubacco [1], Erik Vijgenboom, Christine Gobin, Armand W.J.W. Tepper, Jesús Salgado, Gerard W. Canters *

Leiden Institute of Chemistry, Leiden University, Gorlaeus Laboratories, PO Box 9502, 2300 RA Leiden, Netherlands

Abstract

A scaled-up isolation and purification procedure is described for tyrosinase from *Streptomyces antibioticus*. Kinetic studies of the enzyme catalysed conversion of L-3,4-dihydroxyphenylalanine (L-DOPA) into DOPAchrome show that kojic acid, L-mimosine, *p*-toluic acid and benzoic acid exhibit competitive inhibition with inhibition constants of 3.4, 30, 1.9×10^2 and 8.0×10^2 μM, respectively. Paramagnetic NMR techniques appear well suited to study the binding of inhibitors to the active site. From the variation of the NMR shifts with temperature a value of $-2J = 156 \pm 6$ cm^{-1} is derived for the exchange coupling between the unpaired spins on the two Cu(II) ions in the active site of the met-tyrosinase/kojic acid complex.

Keywords: Tyrosinase; Inhibition; Paramagnetism; NMR; Dinuclear; Copper; Antiferromagnetic coupling

1. Introduction

Phenol oxidases and oxygenases exhibit a large variation in their prosthetic groups and their specificities. Their widespread occurrence in nature testifies to their importance for vital processes in the living cell. Their relevance for industrial purposes is also evident. An intriguing class of these enzymes is formed by the tyrosinases, which are found in the microbial and fungal as well as in the plant and animal kingdoms, where they are responsible for the conversion of monophenols and *ortho*-diphenols to the corresponding *ortho*-quinones. The single piece of solid structural information about tyrosinases available up to date, pertains to the characterization of the active site, which consists of a dinuclear type 3 Cu-centre [1]. Further structural information is limited and based on the homology with the hemocyanins, the 3D-structures of some of which have been reported [2–4]. On the basis of this homology, it was thought that the metal atoms in the active site of tyrosinase are anchored to the protein framework by six histidines [5] (reviewed in Refs. [6–8]), while the nature of a possible bridging group is unclear [2].

As isolated, the Cu_2-centre in tyrosinases predominantly occurs in the oxidized [Cu(II)–

* Corresponding author. Tel.: +31-71-5274256; fax: +31-71-5274349; e-mail: canters@chem.leidenuniv.nl

[1] Present address: Department of Biology, University of Padova, Via Trieste 75, 35131, Padova, Italy.

1381-1177/00/$ - see front matter
PII: S1381-1177(99)00064-8

Cu(II)] form. In this so-called met-tyrosinase, the Cu(II) ions each carry an unpaired electron but the ground state is diamagnetic due to an antiferromagnetic coupling between the electronic spins (reviewed in Refs. [7,8]). In the reduced form of the enzyme, the metal centre occurs in the diamagnetic [Cu(I)–Cu(I)] state, which is able to bind and subsequently activate dioxygen [9].

It was found recently that at room temperature the met-form exhibits paramagnetism due to the presence of a thermally accessible, paramagnetic $S = 1$ state [10]. In the NMR spectrum of the protein, this results in large paramagnetic shifts of the signals deriving from the ligands of the Cu_2-centre. Thus, the active site in principle becomes amenable for detailed structural and mechanistic investigations. In a first paramagnetic NMR investigation of tyrosinase from *Streptomyces antibioticus*, it was found that the Cu ions in the active-centre are ligated by six histidines, indeed, and that in met-tyrosinase the electronic exchange coupling amounts to $-2J = 72 \pm 3\ \text{cm}^{-1}$ [10]. In the chloride bound form, this coupling increases to $200 \pm 8\ \text{cm}^{-1}$, and the proton exchange rate between the ligand histidines and the bulk water diminishes appreciably which may indicate that chloride binding tightens the substrate cavity [10].

In this communication, we report on a study in which the effect of the inhibitors kojic acid, L-mimosine, *p*-toluic acid and benzoic acid (Scheme 1) on the tyrosinase activity is investigated. Partly, in contrast to previous reports, these compounds all exhibit competitive inhibition. It is shown that inhibitor binding can be characterised by means of the paramagnetic NMR techniques mentioned above.

2. Materials and methods

2.1. Strains and plasmids

The host organism for the expression of the tyrosinase, *S. antibioticus* (LMD 86.18), was obtained from the collection of the Kluyver Laboratory of Delft Technical University, The

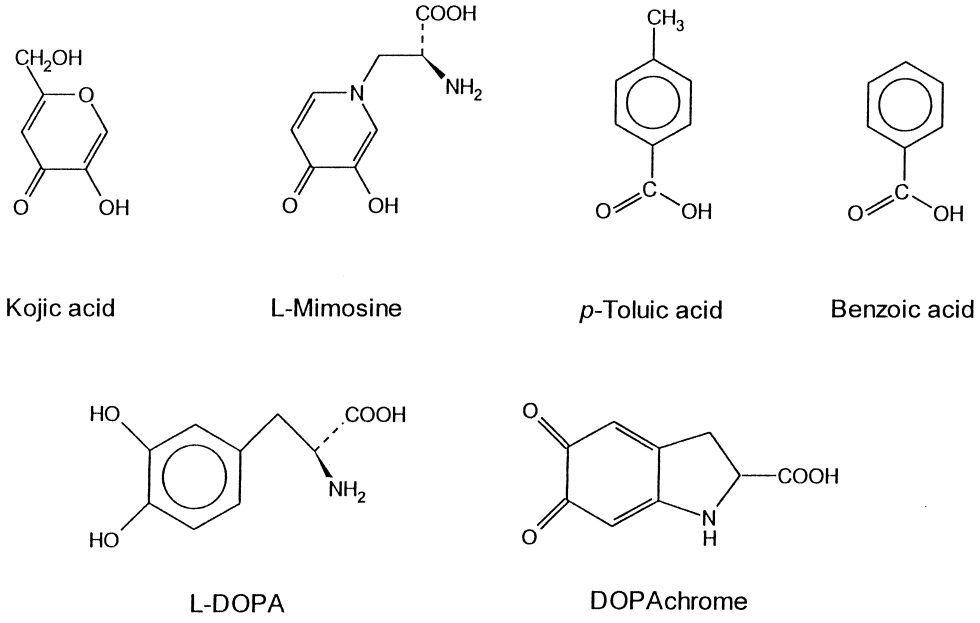

Scheme 1.

Netherlands. Plasmid pIJ703, harbouring the tyrosinase operon (*melC1* and *melC2*) and a thiostrepton resistance marker, was obtained as a kind gift from Prof. Dr. E. Katz [11]. The pIJ703 plasmid was transformed to *S. antibioticus* LMD 86.18 by standard methods [12]. Spores were isolated from *S. antibioticus* pIJ703 cultures growing on MMY-agar plates (per liter of tap water: 4 g maltose, 4 g of Difco yeast extract, 10 g Oxoid malt extract, 17.5 g Difco agar) [13]. Spore stocks were stored in 20% glycerol at -20°C.

2.2. Chemicals

L-DOPA (L-3,4-dihydroxyphenylalanine; Sigma), kojic acid (Sigma), L-mimosine (Sigma), *p*-toluic acid (Aldrich) and benzoic acid (Merck) were used directly from stock. Thiostrepton was a kind gift of Bristol-Myers Squibb.

2.3. Media and culture conditions

Culture medium for the transformed *S. antibioticus* strain was made up of Oxoid tryptone soya broth (30 g/l) and 10% sucrose (w/v) in distilled water and sterilised for 20 min at 120°C. A total of 4 l of culture medium was divided over eight Erlenmeyer flasks (2 l each) containing a stainless steel spring to improve aeration and break up mycelium. To each flask were added 45 μg thiostrepton and $CuSO_4$ to a final concentration of 2 μg/l. Each flask was inoculated with 300 μl of a concentrated spore solution. Flasks were shaken at 300 rpm at 30°C. As tyrosinase is secreted extracellularly by *S. antibioticus* [13], the optimal incubation time could be determined by monitoring the cresolase activity in the medium. Maximum activity was observed after approximately 36 h of growth after which the activity started to decline slowly.

2.4. Protein isolation and purification

The protein isolation and purification protocol basically follows published procedures [13] with some adaptations. Isolation started with separating the medium from the mycelium by centrifugation. At this stage, the medium was pitch black due to large amounts of melanin. The latter was removed by batch treatment of the 4-l supernatant with 400 g wet Whatman DE52 cellulose pre-equilibrated with 10 mM sodium phosphate buffer, pH 6.5. Under these conditions, only melanin binds to the cellulose which was separated from the mother liquor by filtration over a glass filter. The DE52 cellulose treatment was repeated twice. Subsequently, by the addition of salt, the solution was gently brought to 3 M NaCl in 10 mM sodium phosphate, pH 7.2, and incubated with 300 g pre-equilibrated phenyl-sepharose under slow stirring at 4°C for 2–3 h. During this period, the tyrosinase activity of the supernatant slowly reached a minimum indicating binding of the tyrosinase to the sepharose material. The phenyl-sepharose then was poured into a 5×30 cm^2 column and washed with two column volumes of a 3-M solution of NaCl in 10 mM sodium phosphate, pH 7.2. The protein was eluted with a decreasing gradient of NaCl (from 3 to 0 M) in 10 mM sodium phosphate, pH 6.8 and an increasing gradient of ethylene glycol (from 0% to 75% v/v). The fractions containing activity were pooled and concentrated in an Amicon ultrafiltration cell (YM10 filter, Amicon) under nitrogen pressure. By repeated concentration and dilution with 20 mM sodium phosphate buffer, pH 7.0, the ethylene glycol and NaCl were removed from the solution. In the final step, the concentrated tyrosinase solution was poured onto a 2.6×30 cm^2 column containing pre-equilibrated Pharmacia CL-6B CM sepharose in 20 mM sodium phosphate buffer, pH 7.0. The protein was eluted as a single peak by a concentration gradient of sodium phosphate buffer (from 20 to 200 mM). The fractions showing significant activity were pooled and concentrated as described above. The purified tyrosinase was stored at -80°C with 20% (v/v) glycerol as a cryoprotectant. Throughout the purification, the protein solu-

tions were kept on ice to prevent loss of enzymatic activity. The purity of the sample was checked on SDS gel, on which the tyrosinase solution gave a single band at about 30 kDa. On a native 10% agarose gel, a single band was observed (Coomassie blue staining), which coloured dark upon incubation with L-DOPA.

The purified protein is present as a mixture of met-tyrosinase ($\sim 90\%$) and oxy-tyrosinase in equilibrium with the deoxygenated form. During the concentration process, the lower stability of the oxy- and deoxy-tyrosinase results in their conversion to the met-tyrosinase form. The final protein concentration was determined from the optical absorbance at 280 nm in 10 mM sodium phosphate buffer, pH 6.8, by using an extinction coefficient of 8.2×10^4 M^{-1} cm^{-1} [14].

2.5. Enzyme assay

Tyrosinase activity was assayed by using L-DOPA as a substrate [15]. In a typical assay, a concentrated 50 μM tyrosinase stock solution was diluted 100 times in 100 mM phosphate buffer, pH 6.8. An aliquot of 10 μl was mixed in a cuvette containing 20 mM DOPA in 1 ml of 100 mM sodium phosphate pH 6.8 and the increase in absorption at 475 nm due to the formation of DOPAchrome ($\varepsilon_{475} = 3600$ M^{-1} cm^{-1}) [15] was monitored as a function of time. The initial rate was used as a measure for the tyrosinase activity. One unit of enzymatic activity is defined as the amount of enzyme that catalyses the formation of 1 μmol of DOPAchrome per minute at 20°C and pH 6.8 [15].

2.6. Kinetics

Enzyme inhibition studies were carried out by using the same protocol as for the assays, except that also inhibitor was added to the reaction mixture. Four inhibitors were investigated: kojic acid, L-mimosine, *p*-toluic acid and benzoic acid (see Scheme 1). Reaction velocities were measured at three inhibitor concentrations (including zero concentration) on the linear part of the kinetics (initial rates) where the amount of substrate is not the limiting parameter. Results were analysed according to the Lineweaver and Burk (double reciprocal) method which allows for the determination of the Michaelis constant (K_m) and the maximum velocity (V_{max}) [16]. Inhibition kinetics were analysed by determining the initial reaction velocity, V_i as a function of the inhibitor concentration, [I]. Standard analysis yielded the value of the inhibition constant, K_i [16].

2.7. NMR spectroscopy

For the preparation of the NMR samples, a tyrosinase solution was concentrated as described above. In the end, a homogeneous met-tyrosinase solution was obtained as indicated by the absence of an absorption band at 345 nm, which is characteristic of the oxygenated form [17]. The maximum attainable concentration amounted to 600–700 μM (in 100 mM phosphate buffer, pH 6.8). The Cl^--bound species was obtained by adding NaCl up to a concentration of 500 mM.

NMR spectra were recorded at 600 MHz on a Bruker DMX-600 spectrometer. The 1D NMR spectra were measured by applying the super-WEFT pulse sequence [18]. An average of 16 000 scans was required to obtain acceptable signal to noise ratios. The spectra of the inhibitor bound forms were obtained immediately after addition of a small aliquot of a buffered, concentrated inhibitor solution to the NMR sample. Longer incubation times did not result in a change of spectra. Furthermore, there was no decrease of the signal intensity with time, indicating that the inhibitors do not remove the copper from the active site at the concentrations used in the experiment.

Table 1
Tyrosinase activity and recovery for each step during a typical protein purification procedure

Purification steps	Activity[a] (units/ml)	Volume (ml)	Recovery (%)
Culture medium	6.0	4000	100
After centrifugation	5.3	3750	83
After DE52 cellulose treatment	3.5	4300	63
After phenyl sepharose column	24	560	56
After CL-6B CM sepharose column	44.4	290	54

[a]The activity of purified tyrosinase amounts to 1000 (±50) units/mg [15].

The *J*-coupling of the met-tyrosinase/kojic acid complex was determined according to literature methods [19–22], by analysing the paramagnetic shifts of ^{1}H NMR spectra measured at four different temperatures (280, 287, 294 and 301 K).

3. Results

3.1. Protein isolation and purification

A summary of the results obtained in the various steps of the purification procedure is presented in Table 1. As the melanin present in solution during most of the purification steps prevented an accurate determination of the protein concentration, activities in Table 1 are quoted in units/ml instead of units/mg. The total yield of pure protein was determined from

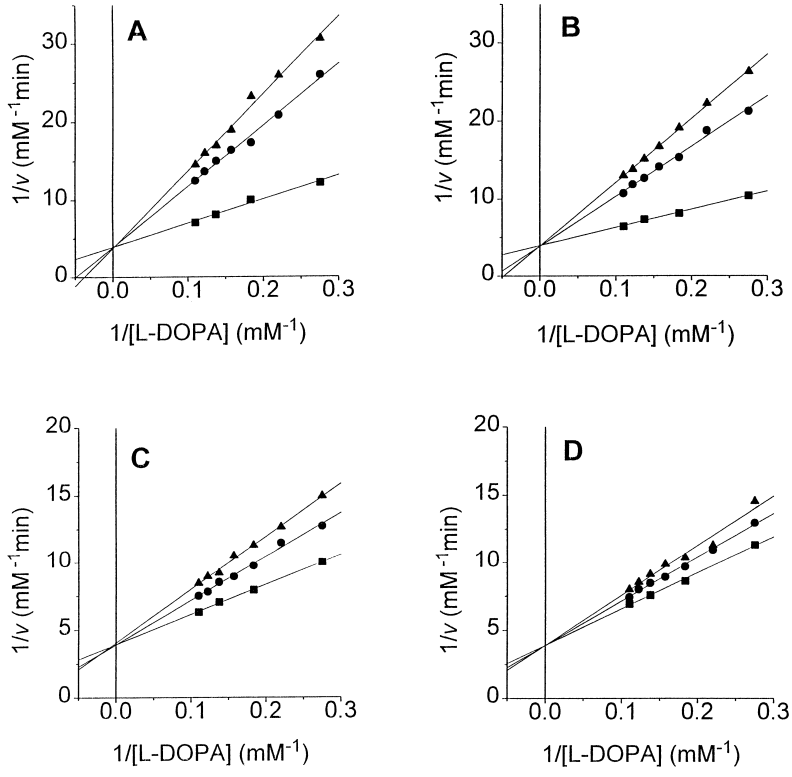

Fig. 1. Double reciprocal plots of the inverse initial rates of conversion of L-DOPA by *S. antibioticus* tyrosinase as a function of inverse substrate concentration in the presence of various concentrations of inhibitors. Measurements were performed as described in Section 2. The straight lines are least squares linear fits to the data points. The following inhibitors were investigated: (A) kojic acid at 0.0 μM (■), 5.0 μM (●) and 7.5 μM (▲) concentration; (B) L-mimosine at 0.0 μM (■), 50 μM (●) and 75 μM (▲) concentration; (C) *p*-toluic acid at 0.0 μM (■), 100 μM (•) and 150 μM (▲) concentration; (D) benzoic acid at 0 μM (■), 150 μM (•) and 300 μM (▲) concentration.

the optical absorbance at 280 nm [14] and varied from 40 to 80 mg per 4 l of culture.

3.2. Kinetics

Double reciprocal plots of the inverse reaction rate of tyrosinase as a function of the inverse substrate concentration (L-DOPA) in the presence of various concentrations of inhibitor are shown in Fig. 1A–D for kojic acid, L-mimosine, *p*-toluic acid and benzoic acid, respectively. The slopes of these plots appear to vary linearly with inhibitor concentration (not shown). From these variations, a value of the inhibitor constant could be extracted [16]. The results are presented in Table 2.

3.3. NMR spectroscopy

A total of 600 MHz ^{1}H NMR spectra of a ~ 600 μM sample of met-tyrosinase in H_2O (100 mM sodium phosphate pH 6.8) at 280 K is shown in Fig. 2, in the absence of inhibitor (A), in the presence of 500 mM NaCl (B), and in the presence of 2 mM kojic acid (C). The positions of the labelled peaks in spectrum C are plotted as a function of temperature in Fig. 3. The data can be fit on the assumption that a paramagnetically excited $S = 1$ state is located at a distance of $-2J$ from the $S = 0$ ground state [22]. A best fit of the data was obtained with $-2J = 156 \pm 6$ cm^{-1}. The drawn lines in Fig. 2 correspond with this value of the exchange coupling. NMR measurements of the met-enzyme complexed with the other inhibitors did not yet

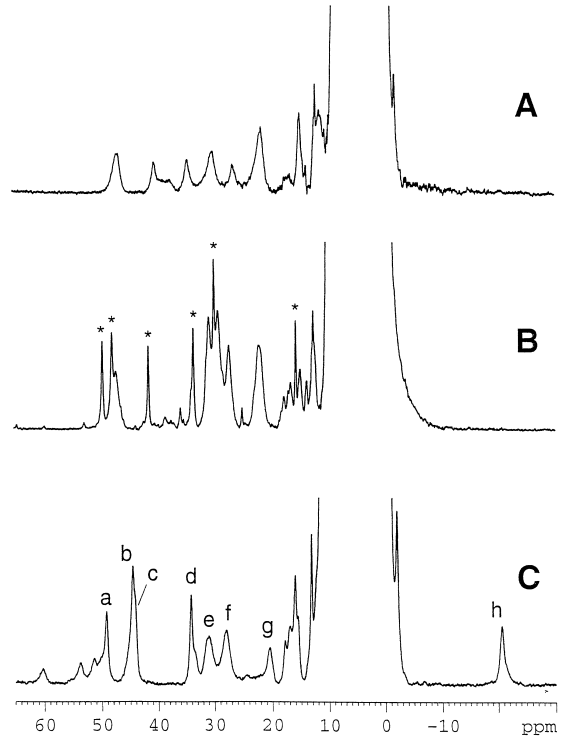

Fig. 2. 600 MHz ^{1}H NMR spectra of a 600–700 μM solution of *S. antibioticus* met-tyrosinase in 100 mM sodium phosphate, pH 6.8 at 280 K. Sixteen thousand transients measured after excitation with a super-WEFT pulse sequence were Fourier transformed after multiplication by a exponential function and baseline corrected. (A) Free met-tyrosinase; (B) same as A but in the presence of 500 mM NaCl; (C) same as A but in the presence of 2 mM kojic acid. The signals labeled with an asterisk derive from the Nδ protons of the six coordinating histidine residues [10]. Signals a, b and d–h in spectrum C were used to determine the value for the *J*-coupling (see Fig. 3).

Table 2
Inhibition constants determined for the four inhibitors used in this study. Measurements were performed in 100 mM sodium phosphate buffer, pH 6.8 and at room temperature. The K_m and V_{max} values of *S. antibioticus* tyrosinase for L-DOPA amount to 8.9 mM and 0.39 mM/min, respectively

Inhibitor	K_i^a (μM)	K_i^b (μM)
Kojic acid	3.4 (0.3)	57[c,d]
L-Mimosine	30 (3)	54[e]
		10[f]
p-Toluic acid	1.95×10^2 (0.18)	500[g]
		80[h]
Benzoic acid	8.0×10^2 (0.9)	700[g]
		18[h]
		14[i]

[a] This work (r.m.s. deviations in brackets).
[b] Literature data.
[c] Previously reported as non-competitive inhibitor [23].
[d] Tyrosinase of undefined *Streptomyces* strain [23].
[e] Mouse melanoma tyrosinase [24].
[f] *Neurospora crassa* tyrosinase [25].
[g] *N. crassa* tyrosinase [26].
[h] Mushroom tyrosinase [27].
[i] *N. crassa* tyrosinase [28].

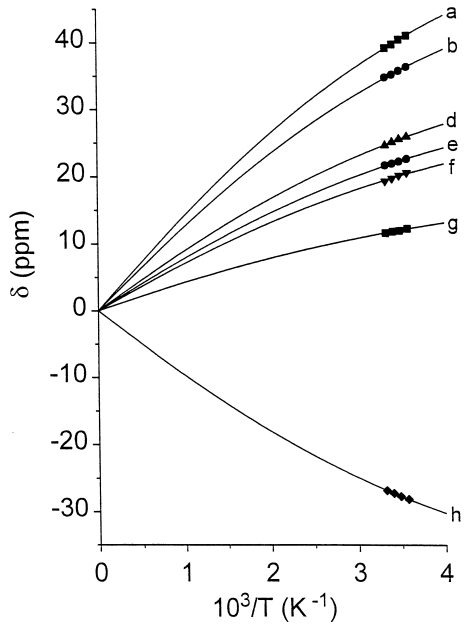

Fig. 3. Variation of the chemical shifts with the inverse absolute temperature, as observed for a number of selected peaks in the 600 MHz NMR spectrum of the kojic acid adduct of *S. antibioticus* met-tyrosinase (see Fig. 2C). The drawn lines are best fits obtained with $-2J = 156 \pm 6\ \mathrm{cm}^{-1}$. Experimental chemical shifts values were corrected for diamagnetic chemical shifts, assumed to be 8 ppm (signals a–g) or 7.5 ppm (signal h).

result in spectra with a signal to noise ratio that was good enough to allow meaningful conclusions.

4. Discussion

4.1. Protein isolation and purification

The present protein isolation and purification procedure is a scaled-up version of a published procedure [13]. The use of a transformed strain of *S. antibioticus*, carrying its own tyrosinase encoding gene on a multi-copy vector (pIJ703), appeared essential for obtaining a sufficient overproduction of the tyrosinase. In our initial efforts to increase the amount of protein per purification, the large amounts of melanin in the culture medium caused problems since the ongoing polymerization reaction would lead to clogged columns and filters. This complication could be obviated by the insertion of a DE52 cellulose-step in the protocol which effectively removes the melanin.

When dissolved in buffer, the purified protein gives a light green solution. This colour is due to the presence of a fraction ($< 10\%$) of the protein in the oxygenated form. The optical spectra of the protein obtained at the end of the purification process show an intense absorption band at 280 nm with a characteristic shoulder at 290 nm and a band at 340 nm previously assigned to a ligand to metal charge transfer transition of the bound O_2 to the copper ion in the active site [17]. The optical spectra of the purified protein are superimposable on the spectra previously presented by Lerch and Ettlinger, for the tyrosinase purified from *Streptomyces glaucescens* [15].

The isolated protein is of the correct size (30 ± 1 kDa; value calculated on the basis of the amino acid sequence: 30,612 kDa [13]) and has the expected substrate specificity. The present procedure provides for sufficient and sufficiently pure protein in a relatively short time (2–3 days) to make the procedure suitable for investigations requiring relatively large amounts of tyrosinase like NMR spectroscopy, although the application of the latter technique is still hampered by the limited solubility ($< 700\ \mu\mathrm{M}$) of the protein.

4.2. Kinetics

The double reciprocal plots in the Fig. 1A–D all exhibit a feature that is characteristic of competitive inhibition, i.e., the regression lines converge to the same point on the vertical axis indicating that $1/V_{\max}$ is not affected by the inhibitor. The NMR spectrum of the kojic acid/enzyme complex also unmistakably shows that the inhibitor binds to the active site of the enzyme (vide infra). The data in Table 2 show a discrepancy with literature data, but at this stage it cannot be excluded that the differences origi-

nate from the fact that the literature data refer to enzymes isolated from other organisms than the one used in the present study.

According to the data in Table 2, the compounds with the smaller inhibition constants share a hydroxy-ketone moiety in their structure, while the two compounds with the larger K_i have a carboxylate function in common. Whether this difference is related to different binding modes is subject of further investigation.

4.3. NMR spectroscopy

The NMR spectra of tyrosinase in the presence and absence of 500 mM chloride (Fig. 2A and B) have been analysed before [10]. The sharp peaks marked with an asterisk in the spectrum of the chloride adduct (Fig. 2B) derive from the Nδ protons of six ligand histidines that coordinate to the Cu ions with their Nε ring atoms [10]. Sharp peaks are missing in the spectrum recorded in the absence of chloride (Fig. 2A), possibly due to a change in the relaxation behaviour of the NMR signals.

A similar conclusion applies when kojic acid binds to the active site. Again a number of sharp peaks are seen in the paramagnetically shifted region of the spectrum (Fig. 2C) although at different positions than in the chloride adduct (see, for instance, signals a, b and d). This indicates that the spin distribution in the active site is affected by the nature of the bound substrate/inhibitor. The high field resonance signal with 1-proton intensity around -20 ppm derives from a proton bound to an atom carrying negative spin density, which we ascribe to one of the ring protons of the kojic acid.

As in the chloride adduct [10], the value of the exchange coupling, $-2J$, in the kojic acid adduct is roughly twice as large as found in the absence of chloride or inhibitor. Apparently, binding of chloride or inhibitor enhances the electronic coupling between the two Cu(II) ions, possibly because of structural changes in the active site. There is no simple way to relate the magnitude of the variation in $2J$ to structural changes in the absence of detailed structural information about the site and the nature of the bridging ligands. If the change in $2J$ that we observe is due to structural variations, they should be small, indeed. For instance, for Cu_2 model compounds in which hydroxide or azide is the bridging ligand, a change in the Cu–O–Cu angle of 1–2° is sufficient to cause a change of $2J$ in the order of 100–200 cm^{-1} [23–25].

5. Conclusion

The conclusions of the present work can be summed up as follows. By using an engineered *S. antibioticus* strain and an improved purification protocol, it is possible to obtain sufficiently large quantities of purified tyrosinase within a moderately short time. This allows for the employment of techniques which are demanding on protein quantities, like NMR.

Kojic acid, L-mimosine, *p*-toluic acid and benzoic acid all show competitive inhibitory kinetics. The presence of either a hydroxy-ketone or a carboxylate functionality in the inhibitors appears to correlate with the magnitude of the inhibition constant.

After the previous demonstration that the active site in the enzyme can be studied advantageously by applying paramagnetic NMR techniques to the met-form of the tyrosinase [10], it now appears that also the enzyme/inhibitor complexes are amenable to this technique.

The temperature variation of the paramagnetic shifts allows for the evaluation of the exchange coupling between the spins on the Cu(II) ions in the active site. The results reported here show that NMR can be fruitfully applied to characterise the binding of inhibitors and transition-state analogues to the enzyme active site. This type of information will contribute to a better understanding of how the ligand geometry and the electronic structure of the active site contribute to the catalytic process.

Acknowledgements

The authors thank Prof. Dr. E. Katz, Georgetown University School of Medicine, Washington, for his gift of the pIJ703 plasmid and for his advice on the molecular biology of the *Streptomyces* strains. They thank Bristol-Myers Squibb for a kind gift of thiostrepton. The assistance of Drs. C. Zaal and Patricia de Kousemaeker in the development and testing of the tyrosinase purification protocol is gratefully acknowledged. This research has been supported by the Netherlands Foundation for Chemical Research (SON) with financial aid from the Netherlands Organisation for Scientific Research (NWO).

References

[1] K. Lerch, Life Chem. Rep. 5 (1987) 221–234.
[2] A. Volbeda, W.G.J. Hol, J. Mol. Biol. 209 (1989) 249–279.
[3] B. Hazes, K.A. Magnus, C. Bonaventura, J. Bonaventura, Z. Dauter, K.H. Kalk, W.G. Hol, Protein Sci. 2 (1993) 597–619.
[4] M.E. Cuff, K.I. Miller, K.E. van Holde, W.A. Hendrickson, J. Mol. Biol. 278 (1998) 855–870.
[5] K. Lerch, M. Huber, J. Inorg. Biochem. 26 (1986) 213–217.
[6] C.W. van Gelder, W.H. Flurkey, H.J. Wichers, Phytochemistry 45 (1997) 1309–1323.
[7] A. Sánchez-Ferrer, J.N. Rodríguez-López, F. García-Canovas, F. García-Carmona, Biochim. Biophys. Acta 1247 (1995) 1–11.
[8] E.I. Solomon, U.M. Sundaram, T.E. Machonkin, Chem. Rev. 96 (1996) 2563–2605.
[9] N. Makino, H.S. Mason, J. Biol. Chem. 248 (1973) 5731–5735.
[10] L. Bubacco, E. Vijgenboom, J. Salgado, A.W.J.W. Tepper, G.W. Canters, FEBS Lett., submitted for publication.
[11] E. Katz, C.J. Thompson, D.A. Hopwood, J. Gen. Microbiol. 129 (1983) 2703–2714.
[12] D.A. Hopwood, M.J. Bibb, K.F. Chater, T. Kieser, C.J. Bruton, H.M. Kieser, D.J. Lydiate, C.P. Smith, J.M. Ward, H. Schrempf, Genetic Manipulation of *Streptomyces*: A Laboratory Manual, The John Innes Foundation, Norwich, 1985.
[13] V. Bernan, D. Filpula, W. Herber, M. Bibb, E. Katz, Gene 37 (1985) 101–110.
[14] P. Jackman, A. Hajnal, K. Lerch, Biochem. J. 274 (1991) 707–713.
[15] K. Lerch, L. Ettlinger, Eur. J. Biochem. 31 (1972) 427–437.
[16] I.H. Segel, Enzyme Kinetics: Behaviour and Analysis of Rapid Equilibrium and Steady-State Enzyme Systems, Wiley, New York, 1993, p. 107.
[17] R.L. Jolley, L.H. Evans, N. Makino, H.S. Mason, J. Biol. Chem. 249 (1974) 335–345.
[18] T. Inubushi, E.D. Becker, J. Magn. Reson. 51 (1983) 128–133.
[19] N.V. Shokhirev, F.A. Walker, J. Phys. Chem. 99 (1995) 17795–17804.
[20] R.C. Holz, J.M. Brink, R.A.R. Rose, J. Magn. Reson. 119 (1996) 125–128.
[21] J.M. Brink, R.A.R. Rose, R.C. Holz, Inorg. Chem. 35 (1996) 2878–2885.
[22] R.C. Holz, J.M. Brink, Inorg. Chem. 33 (1994) 4609–4610.
[23] V.H. Crawford, H.W. Richardson, J.R. Wasson, D.J. Hodgson, W.E. Hatfield, Inorg. Chem. 15 (1976) 2107–2110.
[24] L.K. Thompson, S.S. Tandon, M.E. Manuel, Inorg. Chem. 34 (1995) 2356–2366.
[25] E. Ruiz, P. Alemany, S. Alvarez, J. Cano, J. Am. Chem. Soc. 119 (1997) 1297–1303.
[26] T. Yoshimoto, K. Yamamoto, D. Tsuru, J. Biochem. 97 (1985) 1747–1754.
[27] H. Hashiguchi, H. Takahashi, Mol. Pharmacol. 13 (1977) 362–367.
[28] C. Ruegg, K. Lerch, Biochemistry 20 (1981) 1256–1262.